

## Probing solubilization sites in block copolymer micelles using fluorescence quenching

Andrés F. Olea<sup>a,\*</sup>, Patricio Silva<sup>a</sup>, Irma Fuentes<sup>b</sup>, Francisco Martínez<sup>b</sup>, David R. Worrall<sup>c,\*\*</sup>

<sup>a</sup> Departamento de Ciencias Químicas, Facultad de Ecología y Recursos Naturales, Universidad Andrés Bello, República 275, Santiago, Chile

<sup>b</sup> Facultad Ciencias Físicas y Matemáticas, Universidad de Chile, Santiago, Chile

<sup>c</sup> Department of Chemistry, Loughborough University, Leicestershire LE11 3TU, UK

### ARTICLE INFO

#### Article history:

Received 5 July 2010

Received in revised form

15 September 2010

Accepted 17 September 2010

Available online 29 September 2010

#### Keywords:

Polymer micelles

Block copolymers

Solubilization

Quenching of fluorescence

### ABSTRACT

The solubilization sites provided by micelles formed by a diblock copolymer with one neutral hydrophobic block, polystyrene, and one charged hydrophilic block, poly(acrylic acid) or poly(methacrylic acid), have been studied by fluorescence quenching of pyrene by polar and nonpolar quenchers. Pyrene solubilized into these micelles is distributed between the inner corona and the micelle core. The fraction of pyrene residing in the inner corona is almost unity for star micelles, where the corona-forming blocks are larger than the core-forming blocks, and around 0.5 for crew-cut micelles where the opposite situation prevails. The kinetics of the quenching process depends on the pyrene location, i.e. is static in the micelle core, and largely dynamic in the inner corona at low quencher concentration. The rate constants for fluorescence quenching by nitromethane are shown to increase with increasing pH.

© 2010 Elsevier B.V. All rights reserved.

### 1. Introduction

Amphiphilic block copolymers are known to self-assemble forming micelle-like structures [1]. These polymer micelles provide unique environments for reactions and exhibit the ability to enhance the solubility of hydrophobic molecules in aqueous solution [2,3]. Such properties yield a variety of potential applications including drug delivery [4,5] and environmental cleanup [6]. Various amphiphilic block copolymers composed of a variety of hydrophilic and hydrophobic blocks have been studied. In aqueous solution the hydrophobic blocks form the core of the micelle whilst the hydrophilic blocks form the corona. Poly(ethylene oxide) (PEO) is the most used hydrophilic block in block copolymers for drug delivery systems [7]. However, block copolymers having a charged corona-forming block such as poly(methacrylic acid) (PMA) or poly(acrylic acid) (PAA) have received much attention since their self-assembly behavior can be modulated by pH. The structure of micelles formed by diblock copolymers with one neutral and one charged block has been studied theoretically [8–10] and experimentally [11,12]. Star-type micelles are formed from block copolymers which have corona-forming blocks that are longer than the core-forming blocks [11,13]. On the other hand,

crew-cut aggregates are formed from copolymers with a bulky core and a relatively short corona [14,15]. For star micelles theory predicts two different regions in the corona: the inner corona, which is formed by the PMA chain section where the acid groups are unionized; and the outer corona, composed of sections of PMA chains with a high charge density due to ionized acid groups [8,16]. Thus, in these types of micelles hydrophobic molecules can be solubilized both in the micelle core and in the inner corona.

The release kinetics of hydrophobic molecules from polymeric micelles is a major factor in the potential application of these aggregates as drug delivery systems [17,18]. If the micelle is stable, the location of incorporated molecules within the micelle will strongly affect their release rate and chemical reactivity. Despite the fact that most block copolymers used as drug delivery systems form star-type micelles, the contribution of the inner corona to the solubilization of hydrophobic molecules has not been assessed. The solubilization and release of pyrene and phenanthrene, from crew-cut micelles formed from polystyrene-*b*-poly(methacrylic acid) (PS-*b*-PMA) in aqueous solution have been studied [16]. Results of release kinetics, and fluorescence quenching of the incorporated probe by TI<sup>+</sup> were explained in terms of the three-region model for solubilization of the polycyclic aromatic hydrocarbons. In this work a series of PS-*b*-PAA and PS-*b*-PMA copolymers, which form both star and crew-cut micelles, have been studied by fluorescence techniques, including polarity measurements with pyrene, fluorescence depolarization measurements with perylene, and a quenching study with pyrene and a variety of quenchers. These

\* Corresponding author.

\*\* Corresponding author. Tel.: +44 1509 222567.

E-mail address: [aolea@unab.cl](mailto:aolea@unab.cl) (A.F. Olea).

studies were carried out in aqueous solution to characterize the micelle formed, and to assess the ability of the inner corona to solubilize hydrophobic molecules. The distribution of pyrene between the micelle core and the inner corona has been determined.

## 2. Materials and methods

### 2.1. Polymers

Block copolymers of polystyrene-*b*-poly(*tert*-butyl methacrylate) were synthesized by sequential anionic polymerization of styrene followed by *tert*-butyl methacrylate (t-BuMA) using *sec*-butyllithium as an initiator. Experimental details have been published elsewhere [19]. The diblock copolymers were hydrolyzed to convert the poly(t-BuMA) block into poly(methacrylic acid), in dioxane at 102 °C by refluxing in the presence of HCl. The degree of polymerization of the homopolystyrene and the polydispersity of polymers were determined by GPC. The degree of polymerization of the block copolymers was calculated from the polymer composition, determined by FTIR and <sup>1</sup>H-NMR [20] using a Shimadzu FTIR spectrophotometer, and a Bruker Avance 400 spectrometer.

In addition, some polymers were obtained from Polymer Source and used as received.

The molecular parameters of studied polymers are listed in Table S1. Block copolymers are denoted as PS<sub>*x*</sub>-*b*-PMA<sub>*y*</sub> where *x* and *y* stand for the degrees of polymerization of the PS and PMA blocks, respectively. The relative proportion of these blocks determines the micelle morphology, i.e. copolymers with *x* < *y* form star micelles, whereas copolymers with *x* > *y* form crew-cut micelles [15].

Aqueous dispersions of block copolymers with *x* < *y* were prepared by direct dissolution of polymer in water. Block copolymers that form crew-cut micelles were first dissolved in a common solvent (dimethylformamide, DMF). Then water was added, as precipitant, until the water content reached 50 wt%. Finally, the organic solvent was removed by dialysis of the solution against pure water for 3 days [21].

All aqueous solutions were prepared with distilled and deionized water obtained from an Easy Pure II RF (Barnstead) deionization system.

Pyrene (Aldrich) was recrystallized twice from ethanol. Perylene (Aldrich) was used as received. Samples for fluorescence measurements were prepared by adding a concentrated solution of the probe in THF (1 μL, [pyrene] = 2 mM, [perylene] = 1 mM) to an aqueous polymer solution (2 mL).

### 2.2. Instrumentation

Steady-state fluorescence spectra were recorded on a SLM/Aminco SPF-500C spectrofluorometer by exciting at 337 nm. The ratio *I*<sub>1</sub>/*I*<sub>3</sub> corresponds to the ratio of intensities of peak one (λ = 372 nm) to peak three (λ = 390 nm). Fluorescence anisotropies (*r*) were measured on a Fluoromax 4 spectrofluorometer. The excitation and emission wavelengths were 430 nm and 480 nm, respectively. The fluorescence decay of the singlet excited pyrene was monitored at 400 nm, following excitation with 8 ns pulses at 355 nm from a Lumonics HY200 Q-switched Nd:YAG laser. A description of the time-resolved fluorescence system has been given elsewhere [22].

## 3. Results and discussion

Fluorescence probing of aqueous solutions of block copolymers PS<sub>*x*</sub>-*b*-PMA<sub>*y*</sub>, (Table S1), using pyrene and perylene was carried out with the following aims: to determine the concentration at which the self-assembly of polymer chains starts; to assess the polarity

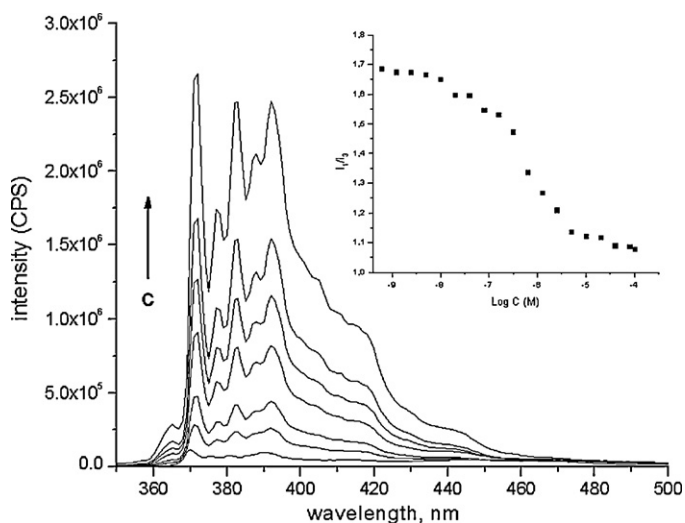


Fig. 1. Fluorescence spectra of pyrene (1.0 μM) in aqueous solutions of PS<sub>129</sub>-*b*-PMA<sub>7</sub> block copolymer. Inset: plot of the ratio *I*<sub>1</sub>/*I*<sub>3</sub> against concentration of block copolymer.

and rigidity of the environment where these hydrophobic probes are located; and to determine the effect of micelle on the quenching process.

### 3.1. Fluorescence of pyrene

Pyrene has been widely used in the study of microheterogeneous systems since its photophysical behavior is highly dependent on the environment in which it is located [23]. In aqueous solutions of micelles or other similar microaggregates, pyrene has been used to report on the micropolarity of the environment in the aggregates [24], and to determine the critical micelle concentration [25].

The fluorescence spectra of pyrene, in aqueous solution of block copolymer, were recorded at different polymer concentrations and at different pH. As polymer concentration increases the fluorescence intensity increases, and the structure of spectrum changes (see Fig. 1). The ratio *I*<sub>1</sub>/*I*<sub>3</sub> of the intensities of the bands that appear at 372 nm (*I*<sub>1</sub>) and 390 nm (*I*<sub>3</sub>) were measured and a plot of *I*<sub>1</sub>/*I*<sub>3</sub> as a function of PS<sub>129</sub>-*b*-PMA<sub>7</sub> concentration is shown in the inset of Fig. 1. It has been shown that this ratio is related to the polarity of the medium where pyrene is located, and an empirical polarity scale has been proposed [23,26]. In polar media this ratio takes high values (in aqueous phase this ratio is equal to 1.90), and it is shown to decrease with decreasing polarity.

The shape of this curve can be explained as follows: in the region of low polymer concentration the value of *I*<sub>1</sub>/*I*<sub>3</sub> corresponds to a very polar medium, which suggests that pyrene is exposed to water. At a certain polymer concentration the value of *I*<sub>1</sub>/*I*<sub>3</sub> decreases steeply, reaching a final constant value. This breaking point corresponds to the concentration at which micelles start to form, i.e. the critical micelle concentration (CMC). Therefore, at high polymer concentration the limiting value of *I*<sub>1</sub>/*I*<sub>3</sub> represents the polarity sensed by pyrene in the hydrophobic sites provided by the polymer micelle. The values of *I*<sub>1</sub>/*I*<sub>3</sub>, at low and high concentrations of block copolymers, are summarized in Table S2.

At high polymer concentrations, the values of *I*<sub>1</sub>/*I*<sub>3</sub> are in the range 0.95 to 1.18 and there is not a clear effect of pH or polymer structure on the polarity sensed by pyrene. A similar value for this ratio has been observed in aqueous solutions of PMA of low molecular weight and was assigned to the PMA chains adopting conformations which provided a hydrophobic microenvironment for pyrene [27]. On the other hand, at low concentrations of copolymers, the values of *I*<sub>1</sub>/*I*<sub>3</sub> are lower than the value measured in

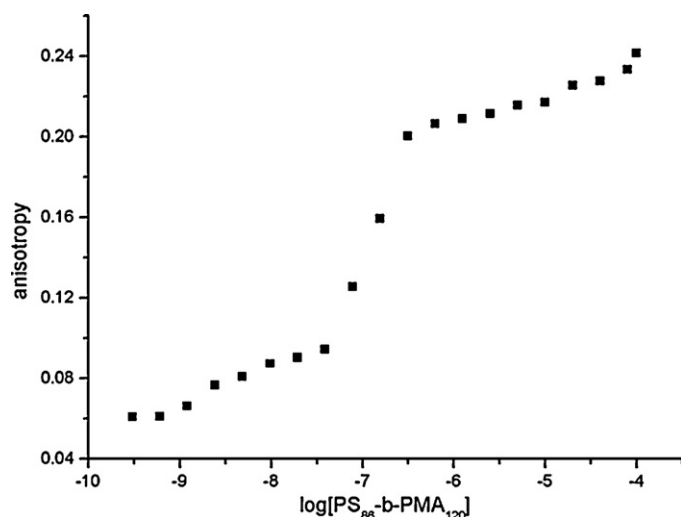


Fig. 2. Fluorescence anisotropy of perylene (0.5  $\mu\text{M}$ ) as a function of  $\text{PS}_{86}\text{-b-PMA}_{120}$  concentration.

aqueous solution. This result suggests that these polymers, even at low concentration, modify the environment sensed by pyrene. Probably, the polymer chain adopts a coiled configuration where the PS residues are protected from water by the hydrophilic charged PMA chain as hypothesized in Ref. [26]. In support of this proposal is the fact that this effect is not observed for block copolymers with short PS blocks. The effect has also been found for block copolymers formed by PS and PEO, where it has been ascribed to pre-micellar aggregates [28].

### 3.2. Depolarization of fluorescence

It has been established that depolarization of fluorescence can be used to determine the viscosity of the environment where the fluorescent probe is located [29]. For example, perylene has been used to determine the microviscosity of micelles [30] and amphiphilic polymers [31]. In Fig. 2 is shown a plot of perylene fluorescence anisotropy as a function of polymer concentration.

The increase of anisotropy with increasing polymer concentration indicates that perylene is being transferred from a fluid to a rigid medium, where reorientation of this molecule on the time scale of fluorescence lifetimes is restricted. This result indicates that the hydrophobic environment provided by polymer micelles is quite rigid, inhibiting mobility of solutes. Anisotropy values measured at high block copolymer concentration are higher than those reported for cationic micelles ( $r=0.038$ ) [30], but similar as those reported for amphiphilic copolymers ( $r=0.14\text{--}0.23$ ) [31].

Based on the changes in emission and excitation spectra of pyrene with polymer concentration several methods to determine the CMC of block copolymers have been proposed [11,28]. The CMC values obtained, for the studied diblock copolymers, by measuring the ratio  $I_1/I_3$  and fluorescence anisotropy of pyrene and perylene, respectively, are in the range  $10^{-6}\text{--}10^{-7}$  M (Table S3). These values are similar to those reported for PS-b-PAA copolymers [11]. The data shows that an increase of the charge density of the corona (high pH) shifts the CMC to higher polymer concentration. This result is ascribed to an increase of polymer solubility with increasing ionization of PMA or PAA blocks.

### 3.3. Quenching of pyrene fluorescence

A first assessment of the location of incorporated probes within the polymer micelles, and the effect of micelles on photophysical reactions, can be made by studying the quenching of pyrene

fluorescence by different molecules. The polymer micelles used here are composed of a hydrophobic PS core and a hydrophilic PAA (PMA) corona, and can therefore provide at least three different sites for solubilization of pyrene: the micelle core, the inner corona, and the outer corona [16,32]. The partition coefficient of pyrene between the aqueous phase and crew-cut micelles formed by PS-b-PMA has been measured, and the high value of this constant indicates that pyrene is completely solubilized into the micelle [11]. Probably, inside the micelle pyrene is distributed between the inner corona and the micelle core [16]. This assumption can be tested using quencher molecules with different polarity. Polar and non-polar quenchers should exhibit different quenching efficiencies depending upon which of the different possible regions of the micelle the substrate is localized. In order to evaluate the effect of micelle morphology and structure of the hydrophilic block, copolymers with similar ratios of  $x/y$  were chosen.

### 3.4. Quenching by nitromethane

Nitromethane is a polar molecule that readily dissolves in water and therefore it would be expected to quench pyrene molecules located in the corona more efficiently than those residing into the micelle core. Results of the steady-state quenching by nitromethane are presented in the form of a Stern–Volmer plot in Fig. 3 for pyrene (1.0  $\mu\text{M}$ ) in an aqueous solution of block copolymers ( $1.0 \times 10^{-5}$  M) at pH 9.1.

It is seen that  $I_0/I$  plots are not linear and show a downward curvature. The downward curvature is generally attributed to quenching of two populations of fluorophores with different accessibilities to quenchers [29]. In this case, the effect is due to unequal accessibility of nitromethane to the corona and micelle core. The fraction of pyrene that resides inside the corona would be more efficiently quenched by nitromethane relative to that localized in the core. As a consequence of this preferential quenching of more exposed pyrene, the polarity sensed by the ratio  $I_1/I_3$  decreases with increasing quenching. Similar behavior has been reported for quenching of pyrene by nitromethane in presence of block copolymers of styrene and acrylamide [33].

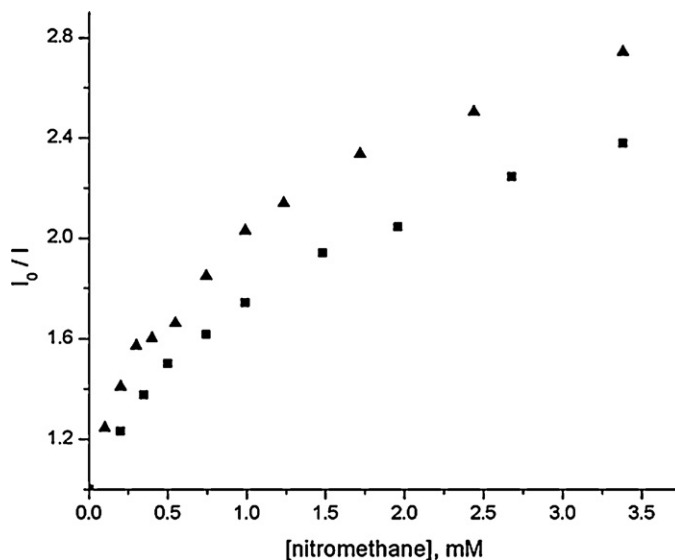


Fig. 3. Stern–Volmer plots for quenching of pyrene (1.0  $\mu\text{M}$ ) by nitromethane in aqueous solution of  $\text{PS}_{26}\text{-b-PMA}_{238}$  (■) and  $\text{PS}_{318}\text{-b-PMA}_{74}$  (▲), at pH 9.1. [Polymer] = ( $1.0 \times 10^{-5}$  M).

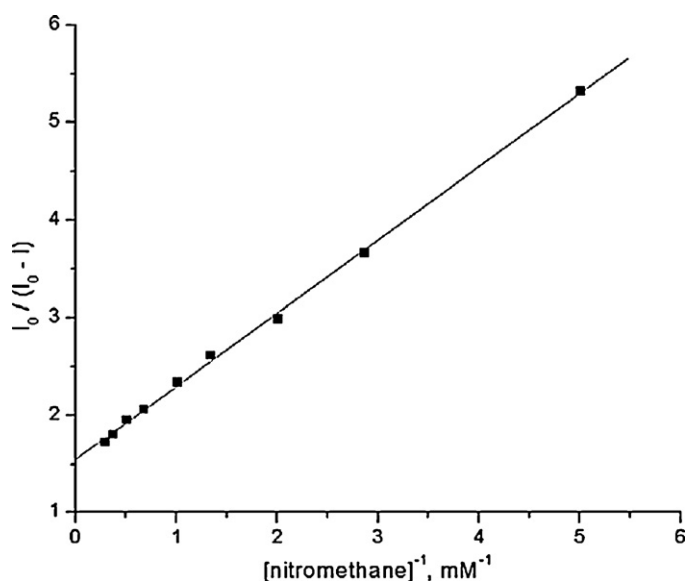


Fig. 4. Modified Stern–Volmer plot for quenching of pyrene (1.0  $\mu\text{M}$ ) by nitromethane in presence of PS<sub>26</sub>-b-PMA<sub>238</sub> ( $1.0 \times 10^{-5}$  M), at pH 9.1.

The fraction of pyrene residing in the corona can be determined using the following equation [29]

$$\frac{I_0}{I_0 - I} = \frac{1}{fK_{SV}[Q]} + \frac{1}{f} \quad (1)$$

where  $K_{SV}$  is the Stern–Volmer constant,  $f$  is the fraction of more accessible pyrene, and  $[Q]$  is the nitromethane concentration. A typical modified Stern–Volmer plot is shown in Fig. 4 for PS<sub>26</sub>-b-PMA<sub>238</sub> at pH 9.1.

The fractions of pyrene that resides in the corona and the  $K_{SV}$  constants are summarized in Table 1.

The data of Table 1 shows that the values of  $f$  are lower for crew-cut micelles, and insensitive to the chemical nature of the hydrophilic polymer block. Also, there is not a clear effect of pH on the fraction of accessible pyrene. It is important to emphasize that, in these micelles, nitromethane is also distributed between the core and the inner corona, and the different quenching efficiencies are a consequence of this distribution. Thus, the  $f$  values indicate that pyrene is mainly residing in the inner corona, and that the fraction of pyrene within the micelle core is not larger than 0.50. These results support the assumption made by Teng et al. [16], that pyrene inside the inner corona is not accessible to  $\text{Ti}^+$ . These authors found that, in crew-cut micelles of PS-b-PMA, the fraction of pyrene accessible to  $\text{Ti}^+$  is 0.23. This low value of  $f$  was attributed to the inaccessibility of the quencher to the inner corona, because of chain crowding and repressed ionization.

Time-resolved fluorescence measurements give further insights to the pyrene distribution. In Fig. 5 are shown the experimental and fitted decay curves for pyrene in aqueous solutions of PS<sub>26</sub>-b-PMA<sub>238</sub> in the presence and absence of nitromethane.

Table 1  
Fractions of pyrene located in the micelle corona and Stern–Volmer constants, at different pH.

Copolymer	pH 4.1		pH 7.2		pH 9.1	
	$K_{SV}, \text{M}^{-1}$	$f$	$K_{SV}, \text{M}^{-1}$	$f$	$K_{SV}, \text{M}^{-1}$	$f$
PS <sub>26</sub> -b-PMA <sub>238</sub>	420	0.81	270	1.0	2050	0.65
PS <sub>32</sub> -b-PAA <sub>263</sub>	180	0.90	375	0.63	1370	0.67
PS <sub>318</sub> -b-PMA <sub>74</sub>	1440	0.58	470	0.47	2830	0.69
PS <sub>144</sub> -b-PAA <sub>47</sub>	750	0.65	1200	0.54	2500	0.52

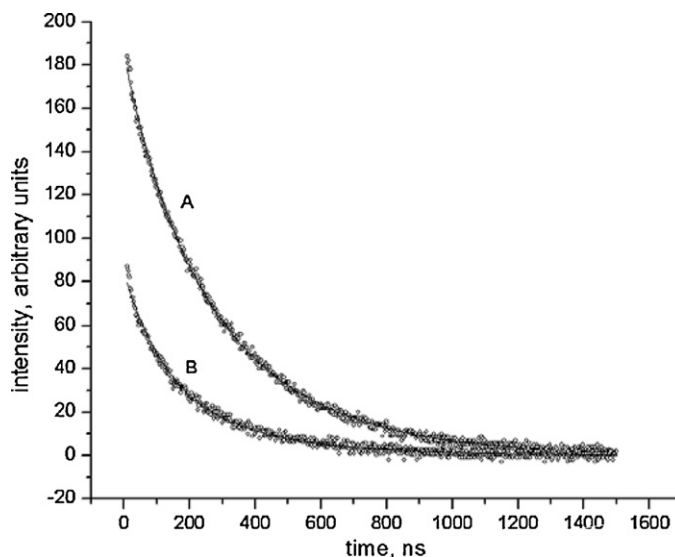


Fig. 5. Fluorescence decays of pyrene (1.0  $\mu\text{M}$ ) in aqueous solutions of PS<sub>26</sub>-b-PMA<sub>238</sub> ( $1.0 \times 10^{-5}$  M) in absence (A) and presence (B) of nitromethane.

As discussed (*vide supra*), in the presence of micelles formed by block copolymers pyrene is located in two different microenvironments and, therefore, in the absence of quenchers, a bi-exponential equation was used to fit the data

$$I(t) = Ae^{-t/\tau_1} + Be^{-t/\tau_2} \quad (2)$$

where  $\tau_1$  and  $\tau_2$  are the lifetimes for pyrene probing these two environments. The longest lifetime  $\tau_1$  is ascribed to pyrene residing in the micelle core, with  $\tau_2$  corresponding to pyrene in the inner corona. The fractions of light emitted from pyrene in the corona relative to the total emission intensity were obtained from the amplitudes as  $q = B/(A + B)$ . The results obtained for PS<sub>32</sub>-b-PAA<sub>263</sub>, at different pH, are given in Table 2.

The data indicates that both lifetimes and  $q$  are only slightly affected by pH. This result suggests that neutralization, produced by increasing pH, probably involves only to the most external carboxylic groups. Therefore, only minor changes are induced in the structure of the core and inner corona. This assumption is validated by the theory, which predicts that for a weak polyacid the neutralization of acid groups in the corona increases with increasing distance from the core/corona interface [34]. In addition, the values of  $q$  and  $f$  agree quite well, and therefore it is possible to conclude that most of pyrene is residing in the inner corona of these polymer micelles.

The difference in amplitudes with and without quencher observed in Fig. 5 suggests that quenching of pyrene emission by nitromethane is not entirely dynamic, and that there is a static contribution. The existence of static quenching suggests that the movements of molecules located in the micelle core are quite restricted, consistent with fluorescence anisotropy measurements (*vide supra*). It is reasonable to assume that sites that prohibit reorientation of perylene also inhibit pyrene and quencher mobility. This result agrees with the extremely low diffusion coefficient of pyrene measured in PS-b-PMA micelles [16].

Table 2  
Lifetimes and fractions of pyrene residing in the inner corona of micelles, formed by PS<sub>32</sub>-b-PAA<sub>263</sub>, at different pH and in the absence of quencher.

pH	$\tau_1$	$\tau_2$	$q$	$f$
4.1	420	270	$0.84 \pm 0.08$	$0.90 \pm 0.13$
7.1	390	290	$0.79 \pm 0.08$	$0.63 \pm 0.06$
9.0	370	220	$0.74 \pm 0.07$	$0.67 \pm 0.05$

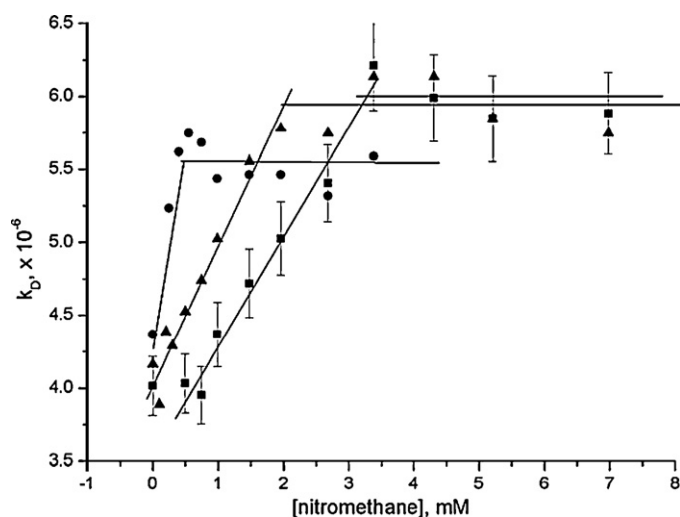


**Fig. 6.** Decay rate constants  $k_D$  ( $=1/\tau_2$ ) of pyrene ( $1.0\ \mu\text{M}$ ) in aqueous solution of PS<sub>32</sub>-b-PMA<sub>263</sub> as function of nitromethane concentration. ■ pH 4.1; ▲ pH 7; ● pH 9. The 5% error on the data is shown as error bars for pH 4.1.

Therefore, the quenching process was assumed to be dynamic for pyrene residing in the corona, and static for pyrene into the micelle core. For fitting of the data, this means that the longer lifetime ( $\tau_1$ ) was kept constant, and  $\tau_2$  was allowed to vary. Therefore the fitting equation is

$$I(t) = Ae^{-t/\tau_1} + Be^{-t/\tau_2} \quad (3)$$

Decay curves fitted with Eqs. (2) and (3) are shown as solid lines in Fig. 5.

A comparison of  $q$  values, obtained in the absence and at high concentration of nitromethane, shows that  $q$  is independent of quencher concentration. The rate constants of dynamic quenching of pyrene in the inner corona were obtained from a plot of  $1/\tau$  against quencher concentration.

Typical plots are shown in Fig. 6 for PS<sub>32</sub>-b-PMA<sub>263</sub> at different pH. It is seen that the rate of decay increases linearly with quencher concentration until a point where the lifetime remains constant. This result indicates that static quenching also takes place in the inner corona. The concentration corresponding with static quenching becoming dominant decreases with increasing pH, indicating that at higher pH the entry of the quencher is more efficient. Quenching rate constants were obtained from the linear region of these plots and are collected in Table 3.

The data show that in all systems the quenching rate constant increases with increasing pH, and that  $k_q$  values are higher in crew-cut micelles than in star micelles. The increase in quenching rate constant is attributed to the opening of the corona and consequently to an increased mobility of pyrene and quencher. The rate constants for quenching of pyrene by nitromethane, in aqueous

solution of PMA at different pH, have been measured previously [35], and the dependence of  $k_q$  with pH is similar to that found in this work for block copolymers. This effect has been ascribed to a pH-induced conformational transition of PAA and PMA chains [36], i.e. at low pH a hypercoiled structure is formed as the acidic form of the carboxylic groups predominates, while at high pH an open structure exists due to electrostatic repulsion of neighboring negative charges. The unfolding of the polymer chain consequently increases the quenching efficiency. At low pH, the  $k_q$  values are higher in block copolymer micelles than in PMA solutions. These results indicate that the corona of the block copolymer micelle is as rigid as the hypercoiled state of PMA. On the other hand, at high pH the values of  $k_q$  are similar to those measured in aqueous solution.

### 3.5. Quenching by non-polar molecules

The fluorescence of pyrene was also quenched by benzophenone, 2,3-dimethylbenzophenone, propyl iodide, and 1,4-dimethylidobenzene. These molecules are expected to be solubilized in the same region as pyrene and, as static quenching was also observed, the quenching was modelled in the same way as for nitromethane. Thus, the decay curves were fitted to Eq. (2).

In all systems, the value of  $q$  increases with increasing degree of quenching, approaching unity. In other words, the decay becomes mono-exponential since the emission of pyrene inside the micelle core is completely suppressed by static quenching. This is an expected result as non-polar quenchers and pyrene are solubilized into the hydrophobic region of the micelle, and static quenching should be more efficient.

The plots of  $k_D$  against quencher concentration are similar to those obtained with nitromethane, but for these molecules the onset concentration of static quenching in the corona is independent of pH. In addition, the rate constants for quenching of pyrene residing in the corona are also independent of pH. This result indicates that the efficiency of quenching, and therefore the mobility of pyrene and the non-polar quenchers, is not affected by change of charge density in the outer corona. This leads to the conclusion that the dependence of  $k_Q$  on pH for the quenching by nitromethane can be ascribed exclusively to enhanced mobility of nitromethane in the outer corona.

## 4. Conclusions

Block copolymers micelles, formed by copolymers having one neutral hydrophobic block and one charged hydrophilic block, provide at least two different sites for solubilization of hydrophobic molecules, i.e. the core and the inner corona. The fraction of pyrene that resides in the inner corona was determined by quenching with nitromethane. The results indicate that this fraction is almost unity for star micelles, and it is lower for crew-cut micelles, but always higher than 0.50. The site of solubilization of pyrene determines the mechanism of quenching by polar and non-polar quenchers. From steady-state and time-resolved measurements it is concluded that pyrene in the core is quenched statically, while quenching of pyrene in the corona is mainly dynamic. In this region static quenching is also observed after a critical concentration of quencher is reached. The structure of the inner corona is determined by the interaction between the unionized polyacid chains. A change of bulk pH affects mainly the most exposed carboxylic groups, i.e. those forming the outer corona. Therefore, the rate constants of quenching by nitromethane increase slightly with increasing pH. This effect is due to changes in nitromethane mobility with changing pH rather than to changes in pyrene mobility or location.

**Table 3**  
Rate constants ( $k_q$ ,  $\times 10^9\ \text{L mol}^{-1}\ \text{s}^{-1}$ ) for quenching of pyrene fluorescence by polar and non-polar molecules, in micelles formed by block copolymers.

Copolymer	pH	Nitromethane	Benzophenone	DMB	Propyl iodide	DMIB
PS <sub>26</sub> -b-PMA <sub>238</sub>	4.1	0.60	2.9	110	0.8	57.0
	7.1	0.95	2.8		1.0	
	9.1	3.0	53.0	57	1.3	30.0
PS <sub>32</sub> -b-PAA <sub>263</sub>	4.1	0.64	42.0	49.0	1.0	38.0
	7.1	0.90	35.0	60.0	0.8	42.0
	9.1	5.6	57.0	60.0	0.6	34.0
PS <sub>318</sub> -b-PMA <sub>74</sub>	4.1	1.1	21.0	130	0.8	39.0
	7.1	6.7	55.0	62.0	0.8	21.0
	9.1	8.8	61.0	72.0	0.5	89.0

## Acknowledgements

This work has been supported by FONDECYT grant 1070371 and The Royal Society. I. Fuentes acknowledges a Ph.D. fellowship from CONICYT.

## Appendix A. Supplementary data

Supplementary data associated with this article can be found, in the online version, at [doi:10.1016/j.jphotochem.2010.09.015](https://doi.org/10.1016/j.jphotochem.2010.09.015).

## References

- [1] P. Alexandridis, B. Lindman, *Amphiphilic Block Copolymers. Self-Assembly and Applications*, Elsevier Science, Amsterdam, 2000.
- [2] P.N. Hurter, T.A. Hatton, *Langmuir* 8 (1992) 1291.
- [3] R. Nagarajan, *Colloids Surf. B* 16 (1999) 55.
- [4] K. Kataoka, A. Harada, Y. Nagasaki, *Adv. Drug Deliv. Rev.* 47 (2001) 113.
- [5] A.V. Kabanov, V.Y. Alakhov, in: P. Alexandridis, B. Lindman (Eds.), *Amphiphilic Block Copolymers. Self-Assembly and Applications*, Elsevier, Amsterdam, 2000, p. 347.
- [6] R. Mosler, T.A. Hatton, *Curr. Opin. Colloid Interface Sci.* 1 (1996) 540.
- [7] H. Otsuka, Y. Nagasaki, K. Kataoka, *Adv. Drug Deliv. Rev.* 55 (2003) 403.
- [8] N.P. Shusharina, I.A. Nyrkova, A.R. Khokhlov, *Macromolecules* 29 (1996) 3167.
- [9] N.P. Shusharina, P. Linse, A.R. Khokhlov, *Macromolecules* 33 (2000) 3892.
- [10] E.B. Zhulina, O.V. Borisov, *Macromolecules* 35 (2002) 9191.
- [11] I.V. Astafieva, X.F. Zhong, A. Eisenberg, *Macromolecules* 26 (1993) 7339.
- [12] E.A. Lysenko, T.K. Bronich, E.V. Slonkina, A. Eisenberg, V.A. Kabanov, A.V. Kabanov, *Macromolecules* 35 (2002) 6351.
- [13] R.L. Xu, M.A. Winnik, F.R. Hallett, G. Riess, M.D. Croucher, *Macromolecules* 24 (1991) 87.
- [14] L.F. Zhang, A. Eisenberg, *J. Am. Chem. Soc.* 118 (1996) 3168.
- [15] G.H. Zhang, K. Khougaz, M. Moffitt, A. Eisenberg, in: P. Alexandridis, B. Lindman (Eds.), *Amphiphilic Block Copolymers. Self-Assembly and Applications*, Elsevier, Amsterdam, 2000, p. 87.
- [16] Y. Teng, M.E. Morrison, P. Munk, S.E. Webber, K. Prochazka, *Macromolecules* 31 (1998) 3578.
- [17] A. Lavasanifar, J. Samuel, G.S. Kwon, *Adv. Drug Deliv. Rev.* 54 (2002) 169.
- [18] C. Allen, D. Maysinger, A. Eisenberg, *Colloids Surf. B* 16 (1999) 3.
- [19] B. Urbano, P. Silva, A.F. Olea, I. Fuentes, F. Martinez, *J. Chil. Chem. Soc.* 53 (2008) 1507.
- [20] X.F. Zhong, S.K. Varshney, A. Eisenberg, *Macromolecules* 25 (1992) 7160.
- [21] Y.S. Yu, L.F. Zhang, A. Eisenberg, *Macromolecules* 31 (1998) 1144.
- [22] A.F. Olea, D. Worrall, F. Wilkinson, S.L. Williams, A.A. Abdel-Shafi, *Phys. Chem. Chem. Phys.* 4 (2002) 1615.
- [23] K. Kalyanasundaram, J.K. Thomas, *J. Am. Chem. Soc.* 99 (1977) 2039.
- [24] A.F. Olea, B. Acevedo, F. Martinez, *J. Phys. Chem. B* 103 (1999) 9306.
- [25] K. Kalyanasundaram, *Photochemistry in Microheterogeneous Systems*, Academic Press, Orlando, 1987.
- [26] D.C. Dong, M.A. Winnik, *Photochem. Photobiol.* 35 (1982) 17.
- [27] A.F. Olea, H. Rosenbluth, J.K. Thomas, *Macromolecules* 32 (1999) 8077.
- [28] M. Wilhelm, C.L. Zhao, Y.C. Wang, R.L. Xu, M.A. Winnik, J.L. Mura, G. Riess, M.D. Croucher, *Macromolecules* 24 (1991) 1033.
- [29] J.R. Lakowicz, *Principles of Fluorescence Spectroscopy*, Plenum Press, New York, 1999.
- [30] M. Shinitzky, A.C. Dianoux, C. Gitler, G. Weber, *Biochemistry* 10 (1971) 2106.
- [31] H. Ringsdorf, J. Venzmer, F.M. Winnik, *Macromolecules* 24 (1991) 1678.
- [32] A. Choucair, A. Eisenberg, *J. Am. Chem. Soc.* 125 (2003) 11993.
- [33] K.C. Dowling, J.K. Thomas, *Macromolecules* 23 (1990) 1059.
- [34] Y.V. Lyatskaya, F.A.M. Leermakers, G.J. Fleer, E.B. Zhulina, T.M. Birshtein, *Macromolecules* 28 (1995) 3562.
- [35] A.F. Olea, J.K. Thomas, *Macromolecules* 22 (1989) 1165.
- [36] A. Katchalsky, P. Spitnik, *J. Polym. Sci.* 2 (1947) 432.